Thin Solid Films 519 (2011) 8347–8350

Contents lists available at ScienceDirect

Thin Solid Films

journal homepage: www.elsevier.com/locate/tsf

NiFe epitaxial films with hcp and fcc structures prepared on bcc-Cr underlayers

Jumpei Higuchi [a,*], Mitsuru Ohtake [a], Yoichi Sato [a], Fumiyoshi Kirino [b], Masaaki Futamoto [a]

[a] Faculty of Science and Engineering, Chuo University, 1-13-27 Kasuga, Bunkyo-ku, Tokyo 112-8551, Japan
[b] Graduate School of Fine Arts, Tokyo National University of Fine Arts and Music, 12-8 Ueno-koen, Taito-ku, Tokyo 110-8714, Japan

ARTICLE INFO

Available online 2 April 2011

Keywords:
NiFe thin film
Metastable hcp crystal structure
Cr underlayer
Epitaxial growth
Single-crystal substrate

ABSTRACT

NiFe epitaxial films are prepared on $Cr(211)_{bcc}$ and $Cr(100)_{bcc}$ underlayers grown hetero-epitaxially on MgO single-crystal substrates by ultra-high vacuum rf magnetron sputtering. The film growth behavior and the crystallographic properties are studied by reflection high energy electron diffraction and pole figure X-ray diffraction. Metastable hcp-NiFe$(1\bar{1}00)$ and hcp-NiFe$(11\bar{2}0)$ crystals respectively nucleate on $Cr(211)_{bcc}$ and $Cr(100)_{bcc}$ underlayers, where the hcp-NiFe crystals are stabilized through hetero-epitaxial growth. The hcp-NiFe$(1\bar{1}00)$ crystal is a single-crystal with the *c*-axis parallel to the substrate surface, whereas the hcp-NiFe $(11\bar{2}0)$ crystal is a bi-crystal with the respective *c*-axes lying in plane and perpendicular each other. With increasing the film thickness, the hcp structure in the NiFe films starts to transform into more stable fcc structure by atomic displacement parallel to the hcp(0001) close packed plane. The resulting films consist of hcp and fcc crystals.

1. Introduction

3*d* ferromagnetic transition metal thin films have been widely studied for applications such as magnetic recording media, magnetic heads, etc. Metastable 3*d* transition metal films have also recently attracted much attention for applications like tunneling magnetoresistance devices [1]. The magnetic properties are greatly affected by their crystal structures.

Ni and Ni – 20 at.% Fe (permalloy) are typical soft magnetic materials and their crystal structures are fcc. hcp-Ni and hcp-NiFe phases are metastable and do not appear in the bulk Ni-Fe phase diagram. hcp-Ni crystals are prepared in the forms of nano-particles and thin films [2–5], whereas there are very few reports on the preparation of hcp-NiFe crystals. Recently, epitaxial thin film growth has made it possible to stabilize metastable structures. hcp-NiFe epitaxial thin films are obtained by molecular beam epitaxy on MgO $(100)_{B1}$ [6], $Au(100)_{fcc}$ [7,8], and $Cr(211)_{bcc}$ [9]. However, parts of the hcp crystals transform into more stable fcc structure when the film thickness exceeds 10 nm [9]. Well-defined hcp-NiFe epitaxial films with moderate thickness are necessary to investigate the basic structural and magnetic properties of metastable hcp-NiFe crystal.

The stability of metastable structure is considered to be influenced by the underlayer material and the underlayer orientation. $Cr(211)_{bcc}$ and $Cr(100)_{bcc}$ have been frequently used as underlayers to prepare hcp-Co$(1\bar{1}00)$ and hcp-Co$(11\bar{2}0)$ epitaxial films with the *c*-axes parallel to the substrate surfaces. The Cr underlayers are also expected to promote the epitaxial growth of hcp-NiFe films with the *c*-axes parallel to the substrate surfaces. In the present study, NiFe films are deposited on $Cr(211)_{bcc}$ and $Cr(100)_{bcc}$ underlayers hetero-epitaxially grown on MgO single-crystal substrates. The film growth, the structure, and the magnetic properties are investigated.

2. Experimental procedure

Thin films were prepared on $MgO(110)_{B1}$ and $MgO(100)_{B1}$ substrates by using an rf magnetron sputtering system where the base pressures were lower than 4×10^{-7} Pa. Before film deposition, the substrates were heated at 600 °C for 1 h in the chamber to obtain clean surfaces. The surface structure was checked by reflection high energy electron diffraction (RHEED). The RHEED patterns observed for the substrates exhibited *Kikuchi* patterns (not shown here), indicating that the surfaces were clean. $Ni_{80}Fe_{20}$ (at.%) and Cr targets of 3 inch diameter were employed. The rf powers for NiFe and Cr targets were respectively fixed at 50 and 40 W, and the Ar gas pressure was kept constant at 0.67 Pa, where the deposition rate was 0.02 nm/s for both materials. The NiFe film compositions were examined by energy dispersive X-ray spectroscopy and the errors were less than 4 at.% from the target composition.

The film layer structure was NiFe(40 nm)/Cr(10 nm)/MgO. 10-nm-thick $Cr(211)_{bcc}$ and $Cr(100)_{bcc}$ underlayers were prepared by hetero-epitaxial growth on $MgO(110)_{B1}$ and $MgO(100)_{B1}$ substrates at 300 °C, respectively. The substrate temperature was used to promote the epitaxial growth of Cr on $MgO(110)_{B1}$ and $MgO(100)_{B1}$. The epitaxial orientation relationships of

$$Cr(211)\left[01\bar{1}\right]_{bcc},\ (211)\left[0\bar{1}1\right]_{bcc}\ ||\ MgO(110)[001]_{B1},$$

* Corresponding author. Tel.: +81 3 3817 1862; fax: +81 3 3817 1847.
E-mail address: higuchi@futamoto.elect.chuo-u.ac.jp (J. Higuchi).

0040-6090/$ – see front matter © 2011 Elsevier B.V. All rights reserved.
doi:10.1016/j.tsf.2011.03.066

$Cr(100)[011]_{bcc}||MgO(100)[001]_{B1}$

were determined by RHEED. The $Cr(211)_{bcc}$ underlayer consisted of two types of variants whose orientations were rotated around the film normal by 180° each other, whereas the $Cr(100)_{bcc}$ underlayer was a single-crystal. 40-nm-thick NiFe films were deposited on the underlayers at room temperature.

The surface structure during rf-sputter deposition process was studied by RHEED. The structural properties were investigated by pole figure, out-of-plane, and in-plane X-ray diffraction (XRD) with Cu-$K\alpha$ radiation ($\lambda = 0.15418$ nm). The magnetization curves were measured by using a vibrating sample magnetometer.

3. Results and discussion

NiFe epitaxial films were obtained on $Cr(211)_{bcc}$ underlayers. Fig. 1(a) and (b) shows the RHEED patterns observed for a $Cr(211)_{bcc}$ underlayer and a 2-nm-thick NiFe film grown on the underlayer, respectively. A clear diffraction pattern corresponding to hcp$(1\bar{1}00)$ texture shown in the RHEED spot map of Fig. 1(d) is observed for the NiFe film. The epitaxial orientation relationship is determined by RHEED as follows,

$$\mathrm{NiFe}\left(1\bar{1}00\right)[0001]_{hcp}\,||\,\mathrm{Cr}(211)\left[01\bar{1}\right]_{bcc},\ (211)\left[0\bar{1}1\right]_{bcc}(\text{Type R}).$$

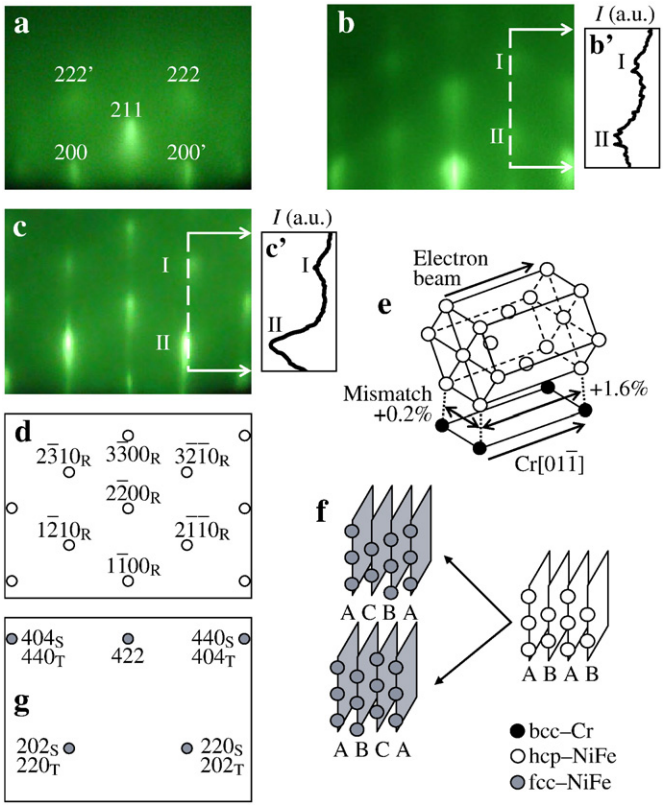

Fig. 1. RHEED patterns observed for (a) a $Cr(211)_{bcc}$ underlayer and (b, c) an NiFe film grown on the underlayer. The film thicknesses are (b) 2 nm and (c) 40 nm. The incident electron beam is parallel to the $MgO[001]_{B1}$ direction. (b', c') RHEED intensity profiles along the dotted lines in (b, c), respectively. (d) RHEED spot map of hcp$(1\bar{1}00)$. (e) Epitaxial orientation relationship and the lattice mismatches of $NiFe(1\bar{1}00)_{hcp}$ || Cr $(211)_{bcc}$. The lattice mismatches are calculated from the lattice constant of bulk Cr crystal and that of hcp-NiFe film determined in the present study. (f) Transformation orientation relationships between the hcp-NiFe$(1\bar{1}00)$ crystal and the fcc-NiFe(211) crystal. (g) RHEED spot map of fcc(211). The symbols, R, S, and T, respectively correspond to the orientation relationships of Types R, S, and T explained in the text. The symbols, A, B, and C, show the stacking sequence of close packed plane.

The NiFe epitaxial film is a single-crystal with a crystallographic orientation relationship with the Cr underlayer schematically shown in Fig. 1(e). When the film thickness is increased, the RHEED spot peak intensity ratio of $2\bar{1}\bar{1}0_R$ (Spot II) to $3\bar{2}\bar{1}0_R$ (Spot I), estimated the RHEED intensity profiles shown in Fig. 1(b') and (c'), increases. The result shows that another pattern is overlapped with the hcp$(1\bar{1}00)$ pattern. In order to examine the possibility of crystal formation other than hcp$(1\bar{1}00)$ crystal, pole figure XRD analysis was performed. Fig. 2(a) and (b) shows the pole figure XRD profiles measured by making the diffraction angle, $2\theta B$, fixed at 47.6° and 44.4°, respectively. The profile of $2\theta B = 47.6°$ shows $NiFe\{1\bar{1}01\}_{hcp}$ reflections, whereas that of $2\theta B = 44.4°$ shows $NiFe\{111\}_{fcc}$ reflections. The result shows that the NiFe film consists of a mixture of hcp and fcc crystals and that the fcc volume in NiFe film is comparable to that of hcp at 40 nm thickness because the XRD peak intensities from fcc and hcp structures are very similar. It is clear that some volume of hcp crystal has transformed into more stable fcc structure. The crystallographic orientation relationships between the hcp and the transformed fcc crystals are determined from the pole figure XRD profiles as follows,

$$\mathrm{NiFe}(211)\left[\bar{1}11\right]_{fcc}||\,\mathrm{NiFe}\left(1\bar{1}00\right)[0001]_{hcp}(\text{Type S}),$$

$$\mathrm{NiFe}(211)\left[1\bar{1}\bar{1}\right]_{fcc}||\,\mathrm{NiFe}\left(1\bar{1}00\right)[0001]_{hcp}(\text{Type T}).$$

In these configurations, the close packed plane of hcp crystal is parallel to that of fcc crystal, as shown in Fig. 1(f). The hcp structure in the NiFe film is apparently transforming into more stable fcc structure possibly by atomic displacement parallel to the hcp(0001) close packed plane. When the transformation orientation relationships are considered, the fcc(211) reflection pattern shown in Fig. 1(g) is expected to be overlapped with the hcp$(1\bar{1}00)$ pattern in the RHEED observed for 40-nm-thick NiFe film.

In order to estimate the lattice constants of the hcp-NiFe crystal formed on $Cr(211)_{bcc}$ underlayer, out-of-plane and in-plane XRD analyses were carried out. Fig. 3(a) and (b)–(c) respectively shows the out-of-plane and the in-plane XRD spectra of the NiFe film grown on $Cr(211)_{bcc}$ underlayer. In the out-of-plane XRD spectrum shown in Fig. 3(a), hcp-NiFe$(1\bar{1}00)$ reflection is clearly observed in addition to the $MgO(110)_{B1}$ and the $Cr(211)_{bcc}$ reflections. The reflection from the transformed fcc-NiFe crystal is not recognized due to that the NiFe(211) plane is parallel to the substrate surface and fcc(211) reflection is a forbidden reflection. The lattice constant, a, of hcp-NiFe crystal is determined from the $NiFe(1\bar{1}00)_{hcp}$ XRD peak angle to be $a = 2 \times d_{NiFe(1\bar{1}00)}/(3)^{1/2} = 0.250$ nm. In the in-plane spectrum shown in Fig. 3(b), hcp-NiFe(0002), fcc-NiFe$(\bar{1}11) + (1\bar{1}\bar{1})$, and bcc-Cr$(01\bar{1}) +$

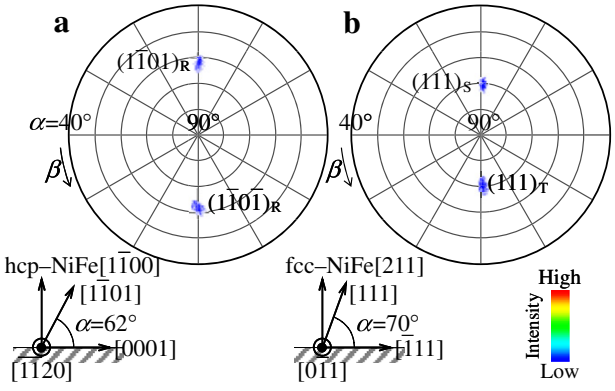

Fig. 2. Pole figure XRD profiles measured by making the diffraction angle, $2\theta B$, fixed at (a) 47.6° and (b) 44.4°. The intensity is shown in a logarithmic scale.